COMMUNICATION

A Cation Concentration Gradient Approach to Tune the Selectivity and Activity of CO_2 Electroreduction

*Wenhao Ren, Aoni Xu, Karen Chan, Xile Hu**

Abstract: The linear scaling relationship of the binding energies of different intermediates limits the catalyst performance in CO_2 electroreduction. Here we demonstrate a cation concentration gradient strategy to promote the activity and tune the selectivity of CO_2 electroreduction, thereby breaking the scaling relationship. In optimal concentrations of the potassium acetate (KAc) electrolyte, Cu, Ag and In catalysts deliver current densities that are 7.1, 3.2, 2.7 times higher than those obtained in 0.5 M KAc for C_2H_4, CO, and formate production, respectively. Increasing the concentration of KAc also changes the selectivity from CO to formate on Ag, and from CO to C_2 products on Cu. *In situ* surface-enhanced Raman spectroscopy and computational simulations reveal that the binding energies of intermediates are changed at different electrolyte concentrations, which is due to a local electrostatic interaction modulated by potassium cations at the electrode surface.

Electrochemical CO_2 reduction reaction (CO_2RR) offers a promising route to produce valuable chemicals in a carbon-neutral energy cycle.[1] A not-too-weak, not-too-strong binding of intermediates on catalysts is desirable to achieve efficient CO_2RR. Unfortunately, the linear scaling relationship of the binding energies of different intermediates poses a performance limit for most catalysts.[2] To overcome this limitation, approaches to selectively favour the adsorption/desorption of certain intermediates are needed. Apart from catalyst design, alkali metal cations have been used to promote the CO_2RR.[3-7] Several interrelated mechanisms have been proposed to explain the cation effects, including electric field, local pH, stabilization of intermediates, and interfacial water.[8-10] Among them, one major theory is that the cation can stabilize reaction intermediates via local electrostatic interactions.[3,11] Given that various CO_2RR intermediates have different dipole moments, it is in principle possible to selectively favour certain intermediates by the cation-induced dipole-field interaction.[3] However, previously cation effects were generally studied at relatively low concentrations of cation (e.g., 0.1 to 2 M) in H-cells. The effects of highly concentrated cations at high current densities based on gas diffusion electrodes are not yet explored.

Potassium acetate (KAc), which has an ultrahigh H_2O solubility, has been used as a water-in-salt electrolyte for high-voltage aqueous metal-ion batteries.[12] This electrolyte can provide a wide electrochemical stability window and potentially suppress the hydrogen evolution reaction (HER).[13] Although a similarly high concentration of KOH is accessible, KOH reacts with CO_2 to form carbonate, and the OH^- enhancement effect cannot be excluded. Based on these considerations, we decided to explore the concentration gradient KAc for CO_2RR at industrial-relevant currents in flow cells. We hypothesize that K^+ cations near the Outer-Helmholtz plane (OHP) can modulate the binding energy of intermediates via electrostatic interactions. As a result, both the activity and selectivity of catalysts can be significantly tuned by altering the concentration of electrolytes. Here we demonstrate the generality of this strategy for CO_2RR on three archetypical catalysts, including Cu, Ag, and In.

Cu, Ag, and In nanoparticles were synthesized by directly reducing Cu^{2+}, Ag^+ and In^{3+} salts with $NaBH_4$ (Fig. S1). To avoid the slow mass transport of CO_2 in H-cells, the electrochemical measurements of CO_2RR were performed in flow cells based on gas diffusion electrodes (GDE). The electrolyte concentration is defined as molar per kg H_2O due to the volume expansion of the concentrated solution. The bulk pH of all KAc electrolytes is controlled at 10 unless otherwise noted.

The cation concentration-dependent CO_2RR activity is shown in Fig. 1a-c. Different from the promotion effect of KOH solution,[14] a rise-and-fall trend of partial currents is observed as electrolyte concentration increases. By changing the electrolyte concentrations, the optimal CO_2RR current densities can be achieved on different catalysts: Cu, Ag and In exhibit partial current densities of 322.7 mA cm^{-2} at -0.8 V (Fig. 1a), 528.9 mA cm^{-2} at -1.1 V (Fig. 1b), and 433.1 mA cm^{-2} at -1.1 V (Fig. 1c) for C_2H_4, CO and formate production, respectively. Without pH control (bulk pH = 8.6), Cu still delivers a j_{C2H4} of 359.3 mA cm^{-2} at -0.88 V and 734.4 mA cm^{-2} at -0.99 V in 2.5 M KAc (Fig. S3). These activity metrics are higher than most catalysts in near-neutral media,[15,16] and are even comparable to many state-of-the-art catalysts in alkaline conditions.[17-19]

Notably, the optimal electrolyte concentration for CO_2RR tends to decrease as the applied potentials increase. For example, the highest j_{C2H4} of Cu at -0.6 V, -0.7 V, and -0.8 V are obtained at 10 M, 7.5 M and 2.5 M, respectively (Fig. 1a). A similar trend is observed on the Ag catalyst (Fig. 1b), where the highest j_{CO} at -0.9 V and -1.0/-1.1 V are obtained at 10 M and 7.5 M, respectively. This trend is consistent with the cation-induced electric field effect, where a lower cation concentration is required at a higher applied potential to balance the surface charge density to achieve the same optimal field strength. The cation effect was then compared among NaAc, KAc, and CsAc (Fig. S4), where the promotion trend follows $Cs^+ > K^+ > Na^+$. This result is consistent with the trend of hydrated ionic radius of these cations ($Cs^+ < K^+ < Na^+$). A smaller hydrated ionic radius leads to a higher concentration of cation near the OHP.[3] A possible anion effect[20,21] is probed by comparing CO_2RR in 0.5 M KAc and 0.25 M K_2SO_4. As shown in Fig. S5 and S6, both the activity and selectivity of Cu and Ag catalysts in these two electrolytes are very similar,

Dr. Wenhao Ren, Prof. Xile Hu
Laboratory of Inorganic Synthesis and Catalysis, Institute of Chemical Sciences and Engineering, Ecole Polytechnique Fédérale de Lausanne (EPFL), ISIC-LSCI, 1015 Lausanne, Switzerland.
E-mail: xile.hu@epfl.ch
Prof. Xile Hu
National Center of Competence in Research (NCCR) Catalysis, EPFL, Lausanne CH-1015, Switzerland
Dr. Aoni Xu, Prof. Karen Chan
Catalysis Theory Center, Department of Physics, Technical University of Denmark, 2800 Kgs. Lyngby, Denmark.

Supporting information for this article is given via a link at the end of the document.

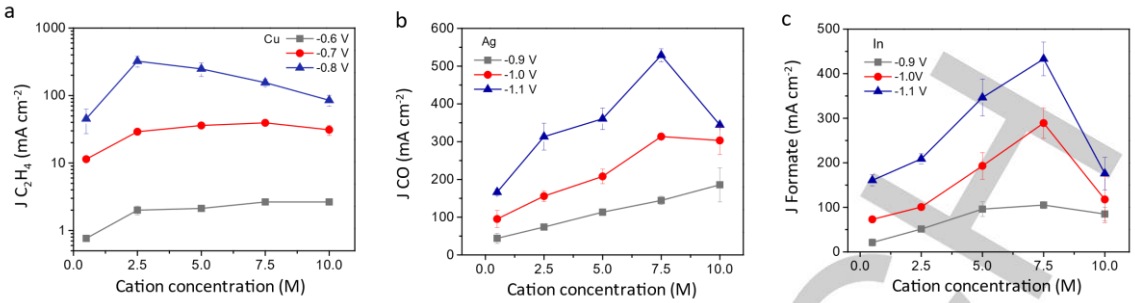

Figure 1. CO_2RR activity. CO_2RR partial current densities as a function of electrolyte concentrations on Cu for C_2H_4 production (a), Ag for CO production (b), and In for formate production (c), respectively.

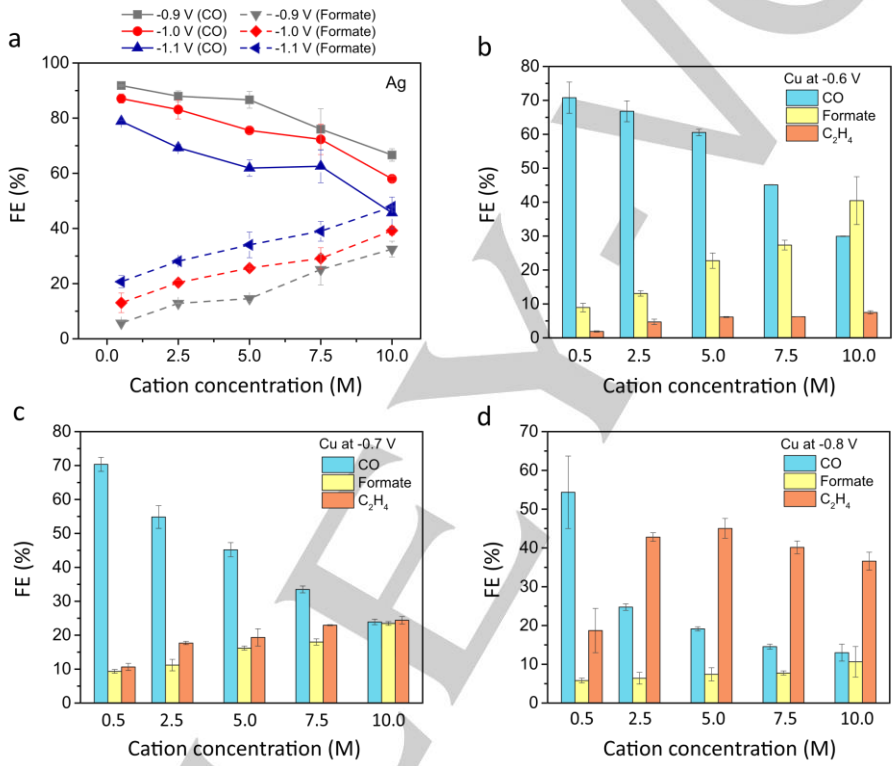

Figure 2. CO_2RR selectivity. Faradaic efficiency (FE) of products on Ag (a), and Cu at -0.6 V (b), -0.7 V (c), and -0.8 V (d) in concentration gradient KAc ranging from 0.5 M to 10 M.

suggesting that the anion effect would be at most minor. Another factor that may alter the CO_2RR performance in concentrated electrolytes (e.g. at 10 M KAc) is mass transport. To reveal the diffusivity in such electrolytes, voltammetry measurements from low (2 mV s^{-1}) to high (500 mV s^{-1}) scan rates were performed (Fig. S7). The currents in 10 M KAc increase slightly with the scan rates, indicative of a minor impact of mass transport owing to the GDE design.[22]

Figure 2a shows the selectivity of Ag under different conditions. Interestingly, with the increase of electrolyte concentration at a given applied potential, or with the increase of applied potential at a given electrolyte concentration, the FE_{CO} decreases and $FE_{formate}$ increases. The $FE_{formate}$ of Ag can reach 47.9% at -1.1 V in 10 M KAc with a $j_{formate}$ of 296.7 mA cm^{-2} (Fig. S8a). A similar phenomenon is observed on Cu at -0.6 to -0.8 V, where the FE_{CO} decreases with the increase of applied potential or electrolyte concentration (Fig. 2b-d). At -0.8 V, the FE_{CO} of Cu decreases about 4 times from 54.4% in 0.5 M KAc to 13.0% in 10 M KAc. Moreover, the increase of FE_{C2H4} is also observed, for example, from 18.6% in 0.5 M KAc to 44.2% in 5 M KAc at -0.8 V. As shown in Fig. S9, a similar trend is observed on Cu at -0.4 V and -0.5 V, where the FE_{CO} decreases and $FE_{formate}$ increases with the increase of electrolyte concentration. The change of j_{C2H4} on Cu at -0.5 V also follows the trend observed at -0.6 V to -0.8 V. For the In catalyst, the $FE_{formate}$ dominates the CO_2RR from 0.5 M to 10 M, and no obvious change can be observed at different applied

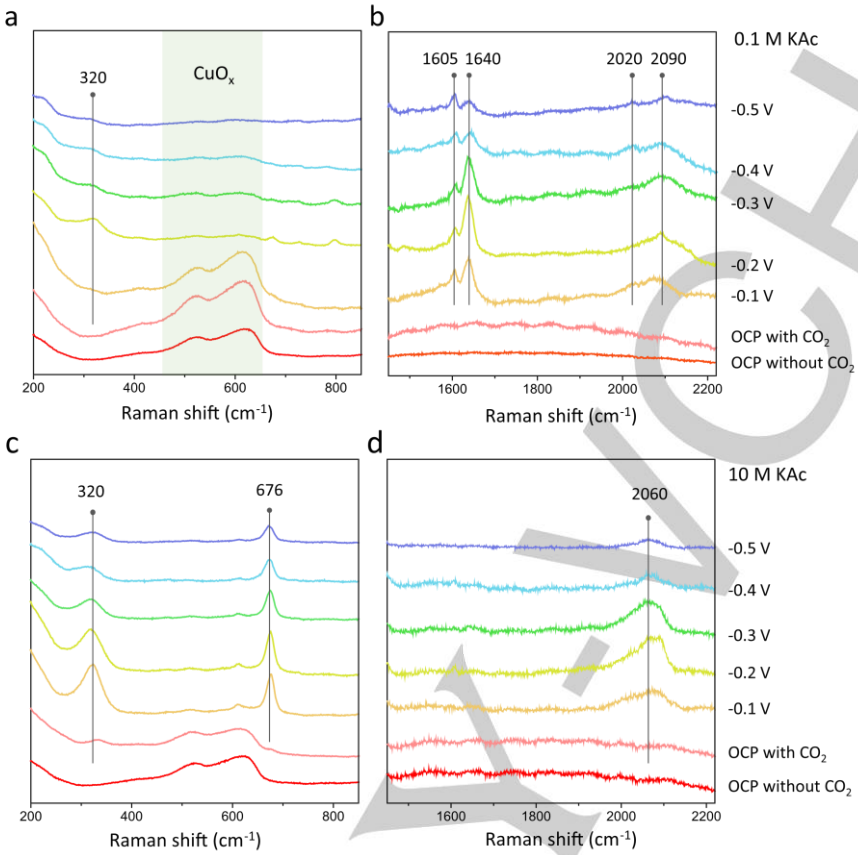

Figure 3. *In situ* surface-enhanced Raman spectra of Cu in 0.1 M KAc (a,b), and 10 M KAc (c,d) from OCP to -0.5 V vs RHE. The assignments of peaks are summarized in Table S2.

potentials or electrolyte concentrations (Fig. S10g-i). Note that although acetate is a potential product from CO_2RR on Cu, in our cases very little if any acetate is formed, as the total FE without considering acetate is close to 100% (Fig. S10).

In situ surface-enhanced Raman spectroscopy (SERS) was used to investigate the adsorption of intermediates on Cu. The first peak at ~320 cm^{-1} can be assigned to the Cu-C bond, either from Cu-CO[23] or Cu-CO_2[24] (Fig. 3a,c). Note that this peak is observable in CO_2-saturated 10 M KAc at OCP (Fig. S11), indicative of the adsorption of CO_2 rather than Cu-CO stretch. This observation is consistent with the CO_2 adsorption theory proposed by Koper and co-workers[11] that the K^+ cation stabilizes the $*CO_2$ via a short-range local electrostatic interaction between K^+–CO_2^-. In addition, Sargent and co-works also pointed out that concentrated cations can lead to a high local concentration of CO_2 on the catalysts surface, and provide strong non-covalent interactions with adsorbed reagent species.[25] This peak, however, cannot be detected in 0.1 M KAc at OCP likely due to the very low K^+ concentration, which also excludes the adsorption of CO_3^{2-}. With the applied potentials, the Cu-C peak in 10 M KAc is constantly larger than in 0.1 M KAc, indicating the stabilization of the $*CO_2$ intermediate during CO_2RR in concentrated electrolytes. This conclusion is further supported by the peak observed at 676 cm^{-1} in 10 M KAc, which was previously attributed to the in-plane bending of δCO_2^- intermediates (Fig. 3c).[24,26] To support the assignment of the peaks at 320 cm^{-1} and 676 cm^{-1}, we measured the SERS spectrum in N_2-saturated KAc (Fig. S12). The peaks at 320 and 676 cm^{-1} are no longer observed, indicating that these peaks are attributed to CO_2-related intermediates.

In 0.1 M KAc, two peaks at 1605 cm^{-1} and 1640 cm^{-1} were observed. To distinguish the H_2O peak, we measured the SERS spectrum in D_2O. As shown in Fig. S13, the peak at 1605 cm^{-1} largely vanished in D_2O, supporting its assignment as the O−H bending peak in H_2O (Fig. 3b). The absence of the 1605 cm^{-1} (H_2O) peak in 10 M KAc could be explained by its strong solvation effect, rendering it a water-in-salt solution with less free H_2O.[12] The peak at 1640 cm^{-1} in 0.1 M KAc has been previously assigned to the ν(C=O) of *COOH.[27,28] Note that the formation of *COOH is the first proton transfer step for the CO_2-to-CO conversion. Hence the observation of the 1640 cm^{-1} peak in 0.1 M KAc is in line with the result that CO is the dominant product in low electrolyte concentrations (Fig. 2b). At 10 M KAc, the peak of *COOH at 1640 cm^{-1} is not observed even though the FE_{CO} is about ~30%. This result might be due to the low coverage of *COOH in 10 M KAc compared with 0.1 M KAc, or due to the rapid conversion of *COOH to CO, which precludes detection by the Raman instrument. From 1950 to 2100 cm^{-1}, the C≡O stretch peaks can be observed in both 0.1 M and 10 M KAc. The difference is the peak positions, where two peaks at ~2020 cm^{-1} (bridged CO) and ~2090 cm^{-1} (CO at isolated defect-like sites

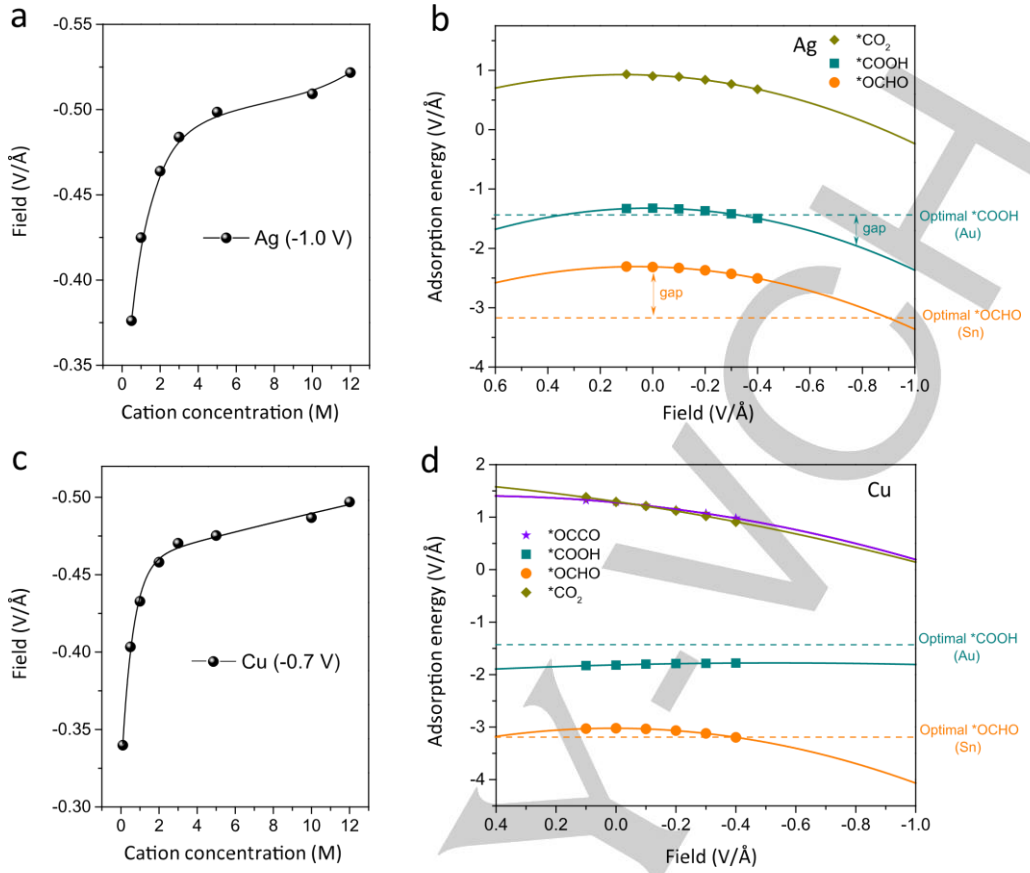

Figure 4. Theoretical simulation. Change of electric field as a function of cation concentrations on Ag at -1.0 V (a), and Cu at -0.7 V (c) at x = a, a is the radius of hydrated K^+. The adsorption energy of intermediates at different electric fields on Ag(111) (b), and Cu(111) (d). The Au and Sn are calculated as references to indicate the optimal adsorption energy of *COOH (CO path) and *OCHO (formate path), respectively.

such as corners or edges) emerge in 0.1 M KAc, and a major peak at ~2060 cm^{-1} (terrace CO) emerges in 10 M KAc.[29] According to previous reports,[29] the terrace CO band at ~2060 cm^{-1} is more correlated with the C-C coupling and C_2H_4 production, while the CO adsorbed on defect sites at ~2090 cm^{-1} is correlated with CO gas formation. The spectroscopic change here again is consistent with the change of selectivity from CO to C_2H_4 observed in electrocatalysis. We could only get reasonable SERS signals at -0.5 V or a less negative potential, because at more negative potentials the formation of gas bubbles severely disturbed the Raman signal, which is commonly encountered.[30] The *in situ* SERS data on Ag is shown in Fig. S14, where the peak intensities are much lower compared to the spectra of Cu. One major difference between the spectra in 0.1 M KAc and 10 M KAc is the peak at 1540 cm^{-1}, which corresponds to the $\nu_{as}CO_2^-$ peak.[24] The detection of $\nu_{as}CO_2^-$ peak in 10 M KAc, but not in 0.1 M KAc, further supports the enhanced adsorption of CO_2 in the concentrated electrolyte.

To understand the change of activity and selectivity on Ag and Cu upon the change of electrolyte concentration, combined mass transport and DFT simulation were conducted to reveal the effect of cation-induced dipole-field interactions. We employed an ionic liquid model to simulate the ion distribution in concentrated electrolytes (e.g. 10 M), which is a continuum model to describe the structure of an electrical double layer in dense liquid by including the crowding effects of finite-sized ions.[31] On both Ag and Cu, the surface cation concentrations (at x = a, a is the radius of hydrated K^+) increase monotonously as increasing the bulk concentration (Fig. S15a,c). Anion (Ac^-) shows an opposite trend with cation in the whole system, until equal to bulk concentration (Fig. S15b,d). Consequently, the field calculated via a modified Poisson equation, increases with local cation concentration at a given potential. For Ag at -1.0 V (Fig. 4a), the field ranges from -0.38 V/Å at 0.5 M to -0.51 V/Å at 10 M. For Cu at -0.7 V (Fig. 4c), the field ranges from -0.34 V/Å at 0.5 M to -0.49 V/Å at 10 M.

The relation between the binding energy of intermediates and the field was then investigated by field-corrected DFT calculations on Ag (Fig. 4b) and Cu (Fig. 4d). On both catalysts, the adsorption of $*CO_2$ is weak at OCP because of the very negative equilibrium potential for $*CO_2^-$ formation.[32-34] With the increase of the field, the adsorption of $*CO_2$ is continuously enhanced on Ag and Cu, which benefits to CO_2RR. This analysis is also supported by the Tafel measurements, where the first electron transfer to $*CO_2$ is the rate-limiting step (RLS) on both Ag (147 mV dec^{-1} at 0.5 M) and Cu (154 mV dec^{-1} at 0.5 M),[7,35] and a decreased Tafel slope is observed as the increase of electrolyte concentration (Fig. S16). Thus, the promotion of $*CO_2$ adsorption is the origin of the boosted CO_2RR activity in concentrated electrolytes. However,

the above analysis cannot explain the trends in selectivity as the *CO_2 adsorption is always the RLS.

To understand the selectivity change between CO and formate on catalysts, we investigate the first proton transfer step for the formation of *COOH (CO path) vs *OCHO (formate path) (Fig. S17). Consistent with previous simulations,[36] Ag shows lower adsorption energy on *OCHO than on *COOH while both *CO_2 → *COOH and *CO_2 → *OCHO conversion are thermodynamically favourable at -1.0 V vs RHE (Fig. S18). Given that the kinetic factors are not captured in the electronic energy calculations, the direct comparison of adsorption energies of *OCHO and *COOH cannot be used to predict the selectivity. We then introduce Au and Sn, which are on the peak positions of CO and formate volcanos respectively, as descriptors for product preference. In low-concentration electrolytes (field < -0.4 V/Å), Ag shows an adsorption energy of *COOH around -1.5 eV, close to the optimal value of Au in CO volcano, while the adsorption of *OCHO is weaker and far from the optimal Sn reference (Fig. 4b). Therefore, CO is the major product on Ag when cation concentration is low and the field is weak. With cation concentration increases, the surface field increases to higher than -0.5 V/Å at -1.0 V_{RHE}. In this region, the adsorption of *OCHO on Ag gradually shifts towards the optimal strength of Sn reference, while the adsorption of *COOH undergoes over-strengthening and is lower than the optimal value. Hence the continuously increased field introduced by dense cation leads to the change of selectivity from CO to formate on Ag. As for Cu, the adsorption of *COOH doesn't show obvious change at different fields, while the adsorption energy of *OCHO shifts towards Sn reference from 0 V/Å to -0.4 V/Å. This trend is consistent with the decrease of FE_{CO} and the increase of $FE_{formate}$ shown in Fig. 2b,c. In addition, the *OCCO adsorption on Cu is greatly enhanced with the increase of the field. The stabilization of *OCCO has the effect of lowering the barrier of C−C bond coupling which is considered as a key step for C_2 product formation,[3] and can be correlated to the enhanced FE_{C2H4} on Cu in concentrated electrolytes.

In addition to the dipole-field interactions, other factors might also contribute to the observed reactivity difference. As shown in Fig. 1 and Fig. S2, the optimal electrolyte concentration for the total current density of CO_2RR is different for the three catalysts. For Ag and In, the highest CO_2RR current densities were obtained at 7.5 M KAc, while for Cu the highest CO_2RR current density was obtained at 2.5 M. This difference might be attributed to water availability. On Ag and In, CO_2RR yields mostly 2-electron reduction products such as formate and CO, which consume only one equivalent of water. On the other hand, for CO_2RR on Cu, a large amount of C_{2+} products are formed, which consume much more water (e.g, eight water molecules are needed for one C_2H_4). The strong solvation in concentrated cations results in less free H_2O in electrolytes as shown in SERS at 1605 cm^{-1} (Fig. 3b,d). [12] As a result, the total CO_2RR current densities peaked at a lower electrolyte concentration on Cu than on Ag and In. The conductivity of electrolytes might be a factor influencing the catalytic activity. However, all the electrochemical measurements are *iR*-corrected. Moreover, the conductivity difference between 2.5 M to 10 M KAc is very small (Table S1). Thus, we do not consider electrolyte conductivity as an important factor that determines the overall activity. This conclusion is further supported by the fact that the highest conductivity of the electrolyte is in 5 and 7.5 M KAc, while the optimal electrolyte concentration for Cu is 2.5 M.

In conclusion, we demonstrate gradient cation concentrations as a universal strategy to promote the activity and steer the selectivity of CO_2 electroreduction on various benchmark electrocatalysts. According to *in situ* SERS and theoretical simulations, the change of selectivity and activity is mostly a result of cation-induced electrostatic interactions on different intermediates. This strategy might be applicable to overcome the scaling limitations in other electrochemical reactions such as CO reduction reactions.

Acknowledgements

The experimental work was supported by the European Union Marie Sklodowska-Curie Individual Fellowships (No. 891545 to W.R.). The simulation work was supported by research grants 9455 and 29450 from VILLUM FONDEN. This publication was created as part of NCCR Catalysis (grant number 180544), a National Centre of Competence in Research funded by the Swiss National Science Foundation.

Author contribution

W.R. and A.X. contributed equally to this work. W.R. performed the synthesis, characterization, and electrochemical tests. A.X. and K.C. conducted the theoretical simulations. All the authors contributed to the data analysis and paper writing. X.H. and K.C. directed the research. The data is available on Zenodo, doi: 10.5281/zenodo.6511898.

Keywords: Cation effect • concentration gradient • electrocatalysis • CO_2 reduction

[1] M. B. Ross, P. De Luna, Y. Li, C.-T. Dinh, D. Kim, P. Yang, E. H. Sargent, *Nat. Catal.*, **2019**, 2, 648-658.
[2] Z. J. Zhao, S. Liu, S. Zha, D. Cheng, F. Studt, G. Henkelman, J. Gong, *Nat. Rev. Mater.*, **2019**, 4, 792-804.
[3] J. Resasco, L. D. Chen, E. Clark, C. Tsai, C. Hahn, T. F. Jaramillo, K. Chan, A. T. Bell, *J. Am. Chem. Soc.* **2017**, 139, 11277-11287.
[4] S. Ringe, E. L. Clark, J. Resasco, A. Walton, B. Seger, A. T. Bell, K. Chan, *Energy Environ. Sci.* **2019**, 12, 3001-3014.
[5] L. D. Chen, M. Urushihara, K. Chan, J. K. Nørskov, *ACS Catal.* **2016**, 6, 7133-7139.
[6] B. Pan, Y. Wang, Y. Li, *Chem Catal.* **2022**, 2, 1267-1276.
[7] J. Gu, S. Liu, W. Ni, W. Ren, S. Haussener, X. Hu, *Nat. Catal.* **2022**, 5, 268-276.
[8] M. M. Waegele, C. M. Gunathunge, J. Li, X. Li, *J. Chem. Phys.* **2019**, 151, 160902.
[9] N. Govindarajan, A. Xu, K. Chan, *Science* **2022**, 375, 379-380.
[10] A. Xu, N. Govindarajan, G. Kastlunger, S. Vijay, K. Chan, *Acc. Chem. Res.* **2022**, 3001-3014.
[11] M. C. Monteiro, F. Dattila, B. Hagedoorn, R. García-Muelas, N. López, M. Koper, *Nat. Catal.* **2021**, 4, 654-662.
[12] L. Suo, O. Borodin, T. Gao, M. Olguin, J. Ho, X. Fan, C. Luo, C. Wang, K. Xu, *Science* **2015**, 350, 938-943.
[13] J. Xie, Z. Liang, Y. C. Lu, *Nat. Mater.* **2020**, 19, 1006-1011.
[14] C. T. Dinh, T. Burdyny, M. G. Kibria, A. Seifitokaldani, C. M. Gabardo, F. P. G. de Arquer, A. Kiani, J. P. Edwards, P. De Luna, O. S. Bushuyev, *Science* **2018**, 360, 783-787.
[15] S. Verma, Y. Hamasaki, C. Kim, W. Huang, S. Lu, H.-R. M. Jhong, A. A. Gewirth, T. Fujigaya, N. Nakashima, P. J. Kenis, *ACS Energy Lett.* **2017**, 3, 193-198.
[16] X. Zhang, J. Li, Y. Y. Li, Y. Jung, Y. Kuang, G. Zhu, Y. Liang, H. Dai, *J. Am. Chem. Soc.* **2021**, 143, 3245-3255.

[17] C. T. Dinh, F. P. García de Arquer, D. Sinton, E. H. Sargent, *ACS Energy Lett.* **2018**, 3, 2835-2840.
[18] J. Gu, C. S. Hsu, L. Bai, H. M. Chen, X. Hu, *Science* **2019**, 364, 1091-1094.
[19] S. Ren, D. Joulié, D. Salvatore, K. Torbensen, M. Wang, M. Robert, C. P. Berlinguette, *Science* **2019**, 365, 367-369.
[20] Y. C. Hsieh, S. D. Senanayake, Y. Zhang, W. Xu, D. E. Polyansky, *ACS Catal.* **2015**, 5, 5349-5356
[21] M. C. Monteiro, M. F. Philips, K. J. P. Schouten, M. Koper, *Nat. Commun.* **2021**, 12, 4943.
[22] G. Marcandalli, M. Villalba, M. T. Koper, *Langmuir* **2021**, 37, 5707-5716.
[23] F. Li, Y. C. Li, Z. Wang, J. Li, D. H. Nam, Y. Lum, M. Luo, X. Wang, A. Ozden, S. F. Hung, *Nat. Catal.* **2020**, 3, 75-82.
[24] I. V. Chernyshova, P. Somasundaran, S. Ponnurangam, *Proc. Nati. Acad. Sci.* **2018**, 115, E9261-E9270.
[25] M. Liu, Y. Pang, B. Zhang, P. De Luna, O. Voznyy, J. Xu, X. Zheng, C. T. Dinh, F. Fan, C. Cao, *Nature* **2016**, 537, 382-386.
[26] D. H. Gibson, *Coord. Chem. Rev.* **1999**, 185, 335-355.
[27] W. Shan, R. Liu, H. Zhao, Z. He, Y. Lai, S. Li, G. He, J. Liu, *ACS Nano* **2020**, 14, 11363-11372.
[28] D. Bohra, I. Ledezma‐Yanez, G. Li, W. de Jong, E. A. Pidko, W. A. Smith, *Angew. Chem.* **2019**, 131, 1359-1363.
[29] H. An, L. Wu, L. Mandemaker, S. Yang, J. De Ruiter, J. Wijten, J. Janssens, T. Hartman, W. van der Stam, B. M. Weckhuysen, *Angew. Chem. Int. Ed.* **2021**, 60, 16576-16584.
[30] Y. Yang, S. Ajmal, Y. Feng, K. Li, X. Zheng, L. Zhang, *Chem. Eur. J.* **2020**, 26, 4080-4089.
[31] M. Z. Bazant, B. D. Storey, A. A. Kornyshev, *Phys. Rev. Lett.* **2011**, 106, 046102.
[32] A. Wuttig, M. Yaguchi, K. Motobayashi, M. Osawa, Y. Surendranath, *Proc. Nati. Acad. Sci.* **2016**, 113, E4585-E4593.
[33] X. Liu, L. Sun, W. Q. Deng, *J. Phys. Chem. C* **2018**, 122, 8306-8314.
[34] B. A. Rosen, A. Salehi-Khojin, M. R. Thorson, W. Zhu, D. T. Whipple, P. J. Kenis, R. I. Masel, *Science* **2011**, 334, 643-644.
[35] W. Deng, P. Zhang, B. Seger, J. Gong, *Nat. Commun.* **2022**, 13, 803.
[36] J. T. Feaster, C. Shi, E. R. Cave, T. Hatsukade, D. N. Abram, K. P. Kuhl, C. Hahn, J. K. Nørskov, T. F. Jaramillo, *ACS Catal.* **2017**, 7, 4822-4827.

COMMUNICATION

A cation concentration gradient approach is developed to promote the activity and tune the selectivity of CO_2 electroreduction on three archetypical catalysts. This approach provides a new strategy to break the linear scaling relationship of the binding energies of different catalytic intermediates via cation induced dipole-field interactions. @HuLab_EPFL

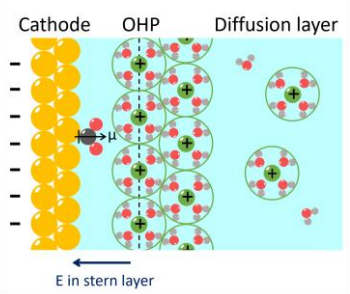

*Wenhao Ren, Aoni Xu, Karen Chan, Xile Hu**

Page No. – Page No.

A Cation Concentration Gradient Approach to Tune the Selectivity and Activity of CO_2 Electroreduction